SOLAR PANEL THERMAL CYCLING TESTING
BY SOLAR SIMULATION AND INFRARED RADIATION METHODS

Hubert E. Nuss*

ABSTRACT

For the solar panels of the European Space Agency (ESA) sa-
tellites OTS/MAROTS and ECS/MARECS the thermal cycling tests
were performed by using solar simulation methods. The perform-
ance data of two different solar simulators used for these tests
and the thermal test results are described. The solar simul-
ation thermal cycling tests for the ECS/MARECS solar panels were
carried out with the aid of a rotatable multipanel test rig by
which simultaneous testing of three solar panels was possible.
As an alternative thermal test method the capability of an in-
frared radiation method was studied and infrared simulation
tests for the ultralight panel (ULP) and the INTELSAT V solar
panels were performed. The setup and the characteristics of
the infrared radiation unit using a quartz lamp array of approx.
15 m^2 and LN2-cooled shutter and the thermal test results are
presented. The irradiation uniformity, the solar panel temper-
ature distribution, temperature changing rates for both test
methods are compared. The results indicate the infrared simul-
ation is an effective solar panel thermal testing method.

INTRODUCTION

Thermal vacuum tests are required for qualification and ac-
ceptance of spacecraft subsystems. The purpose of qualification
tests is to prove the subsystem design by checking its perform-
ance capability under thermal vacuum conditions more severe
than predicted for orbit. The aim of the more severe temper-
ature stress is to demonstrate design safety margin and to ac-
celerate failure in marginal design. The objective of the ac-
ceptance tests is to demonstrate the performance of the sub-
systems of proven design in the temperature range expected in
flight and to verify the workmanship according to flight stan-
dard quality. The cycling between temperature extremes is to
induce temperature gradients in the subsystem thereby permit-
ting observation of operation at other than stabilized condit-
ions.

Thermal vacuum facilities are currently available with
four distinct types of energy control: temperature controlled
shrouds, solar simulators, infrared radiators, surface blanket
heaters.

*Industrieanlagen-Betriebsgesellschaft mbH (IABG), Space Divis-
ion, D 8012 Ottobrunn, West Germany.

The development of infrared simulators with tungsten fila-
ment quartz lamps (refs. 1 to 4) and other methods for infrared
simulation (carbon cloth heat post, fluid controlled panels,
thermal canister, electrical heaters) were described in several
papers (refs. 5 to 8). The application of the different methods
for thermal balance testing was investigated in these studies
and the performance data, testing philosophy, and cost effect-
iveness were compared (refs. 9 to 14).

For satellite programmes thermal vacuum tests have to be
performed for a number of units according to the same specific-
ation. It is especially true for acceptance testing of the
different solar panels of communication satellite's solar array.
The cost effectiveness of solar panel thermal testing can be im-
proved by testing simultaneously more than one panel. In this
paper the development of an infrared radiation unit for simul-
taneous testing of three solar panels is described. The per-
formance data and operational conditions of the infrared radiat-
or setup were studied.

Thermal cycling test results and cost effectiveness for
infrared simulation, for solar simulation for one solar panel,
and for multi-panel solar simulation are compared in the follow-
ing.

1. TEST REQUIREMENTS AND FACILITIES

Thermal vacuum testing of solar panels can be performed
by irradiating the panel front side by a solar simulation or an
infrared simulation setup. By radiation to LN2-cooled shrouds
the temperature gradients through the panel and the temperature
changing rates during the transient phases are similar to the
expected orbit conditions.

The main test requirements for solar panel thermal cycling
tests for different programmes are summarized in Table I. In
general the primary requirement for solar panel thermal testing
by solar simulation methods is the specification of the solar
irradiance to be simulated during test. For the ECS/MARECS
solar panel tests this irradiance was defined equivalent to a
definite value of the open voltage readout during the sunphases
of the thermal cycling test. For the infrared radiation methods
the equilibrium temperatures were specified and therefore the
power of the infrared radiators had to be adjusted to values to
achieve the temperatures required.

1.1 Solar Simulation Facility (Fig. 1 and 2)
The solar panel thermal cycling tests for the OTS/MAROTS
programme were performed in the 3m-space simulation facility of
IABG (ref. 16). The facility is equipped with an LN2-cooled
shroud of 3 m diameter and 7 m length. The solar simulator is
an off-axis system. The radiation is performed by four 25 kW
and five 6.5 kW Xenon Arc lamps. The light is collected in
elliptical mirrors, folded by a plane mirror system to a collim-
ation mirror which directs the radiation into the reference
plane. By means of a light integrator the radiation of the dif-
ferent light sources is superimposed, hence improving the uni-
formity in the reference plane.

The collimation mirror consists of about 1000 adjustable mosaic elements and was adjusted to irradiate a reference plane of 1.9 m diameter, which was sufficient for the dimensions of the solar panels with 1.31 m width and 1.45 m height. The uniformity measurements showed a maximum deviation from the mean value of radiation intensity in the reference plane of $\pm$ 8 %. For simulation of the cold phases an LN2-cooled shutter between collimation mirror and test article shielded the simulated solar radiation.

The relatively low overall efficiency of the solar simulator was due to the fact that the solar simulator was in a modification phase which was not completed when the tests had to be performed.

The ECS/MARECS solar panel thermal cycling tests were carried out in the 3m-space simulation facility with the complete modified solar simulator implemented (Fig. 2). Compared to the original design the folding mirror system for the modified solar simulator could be deleted. The solar simulator was equipped with an integrator adjusted to the efficient operation of five 25 kW Xenon Arc lamps. The mosaic mirror was exchanged by a segment mirror consisting of 37 elements. Due to the optical system modification a solar beam diameter of 2.4 m in the reference plane and an overall efficiency of the solar simulator of approximately 10 % could be achieved. For the ECS/ MARECS solar panel thermal cycling tests the facility was equipped with a rotatable multipanel test rig of triangular shape (ref. 21). By this additional device the cost effective simultaneous testing of 3 solar panels was possible: one panel being irradiated by the solar simulator while for the other two a coldphase was simulated.

1.2 Infrared Radiation Facility
(Fig. 3, 4, 5)

The thermal vacuum tests for the INTELSAT V solar panels (dimensions 1.65 m width, 1.91 m height) were carried out in the thermal vacuum facility 3.5 m-TVA of IABG (ref. 18). The facility is equipped with a GN2-cooled shroud of 3.5 m diameter and 6.3 m height. For the infrared simulation thermal cycling tests the facility was furnished with an infrared radiation unit with quartz-line lamps and a liquid nitrogen-cooled, movable shutter (Fig. 3 and 4). The lamp array can be shielded during the cold-phase by moving the LN2-cooled shutter in front of the lamp radiators. The infrared radiation unit consists of three lamp array modules with a total number of 300 quartz-line lamps (nominal power 500 W each). Fig. 3 shows a schematic sketch of two modules of the lamp array used for irradiating two solar panels. For the third solar panel a third lamp array module on the rear side of the two exhibited ones was used. In between the first two and the third lamp array module an LN2-cooled shroud is located to minimize the radiation of not LN2-cooled surfaces to the panels during coldphase. By 150 electrical control units and power supplies the 150 lamp pairs can be controlled separately.

320

For the thermal vacuum cycling tests of the ultralight panel (ULP, dimensions 1.1 m width and 3.22 m height) (ref. 19) two lamp array modules as shown in Fig. 3 were used.

The primary requirements for an infrared radiator setup to be applied for thermal cycling tests are optimum uniformity of irradience in the test plane and minimum blockage of cold shroud during the coldphases. The blockage of the shroud was reduced by the LN2-cooled shutter as shown in Fig. 4. By measuring the irradiance distribution before the test and adjusting the different control units the irradiance uniformity was optimized.

To monitor the irradiance distribution of the infrared lamp array modules a solarcell sensor of 16 cm^2 surface area was moved vertically and horizontally in the testplane. A typical readout of the sensor measured by scanning along a distance of approximately 5000 mm is shown in Fig. 5. The result of the evaluation of a total number of 765 measured extreme values for the three infrared lamp array modules is given in Table II. This Table indicates that for the testplane of 15 m^2 an irradiance uniformity of $\leq \pm 10$ % could be achieved with approx. 75 % of the measuring points within the range of $\leq \pm 5$ %.

2. TEST RESULTS

The temperature T_p of a solar panel in a space simulation facility is described by the following equation:

$$mc \frac{T_p}{dt} = \alpha FI - \sigma e \varepsilon F (T_p^4 - T_{sh}^4) \qquad (1)$$

mc   : Thermal capacity of test article

$\frac{dT_p}{dt}$: Temperature change of test article with time

I, F   : Irradiance and surface area, respectively

σ : Stefan-Boltzmann-Constant

e, T_{sh} : Viewfactor to shroud and shroud temperature, resp.

ε, α : Emissivity and absorptivity, respectively

The solar panel thermal equilibrium temperature T_E can be derived from equation 1:

$$T_E = \sqrt[4]{\frac{I\alpha}{2\sigma\varepsilon} + T_{sh}^4} \qquad (2)$$

From equation 2 the relative temperature change $\Delta T_E/T_E$ due to a relative intensity variation $\Delta I/_I$ can be calculated (ref. 20):

$$\frac{\Delta T_E}{T_E} \approx \frac{1}{4} \cdot \frac{\Delta I}{I} \qquad (3)$$

Taking into account the irradiation uniformity and the heat conductivity in the panel surface (characterized by the expression λF_{12}) the following expression for the temperature change ΔT_{E1} is found from equation 1:

$$\Delta T_{E1} = \frac{\alpha}{8\,\sigma\,\varepsilon\,T_{E1}{}^3 + \dfrac{\lambda F_{12}}{F}}\,\Delta I \qquad (4)$$

For the transition from warmphase to coldphase from equation 1 the ratio f of the slopes of the temperature - time - plotts for solar simulation and infrared simulation can be derived:

$$f = \frac{dT_p/dt\,\big|solar}{dT_p/dt\,\big|IR} = \frac{T_p{}^4 - T_{sh1}{}^4}{T_p{}^4 - T_{sh2}{}^4 - \dfrac{\varepsilon_1 F_1 e_1}{2\,\varepsilon F\,e}\,T_1{}^4} \qquad (5)$$

For the infrared radiation method surface parts of the lamp array which are not completely covered by the LN2-cooled shutter are taken into account by including an irradiance of an emissivity ε_1, of a viewing factor e_1, of an area F_1 and of a temperature T_1.

2.1 Solar Panel equilibrium Temperature Distribution

In Fig. 6 a typical transient phase for solar simulation thermal cycling is exhibited. The temperatures on the solar panel frontside were measured in the range $61 \pm 4^\circ C$. According to equation 2 an equilibrium temperature of $T_E = 60^\circ C$ can be calculated. By using equation 3 and a value of $\pm 8\%$ for the irradiance uniformity a maximum temperature variation of $\pm 7^\circ C$ is estimated. The measured temperature uniformity of $\pm 4^\circ C$ can be interpreted by the effect of heat conductance in the panel surface as described by equation 4.

A typical transient phase for infrared simulation cycling tests with three solar panels is plotted in Fig. 7. The temperatures on the three solar panels were measured in the range $85 \pm 5^\circ C$. The lamp array modules with 300 radiators were operated with a total power of 39 kW on a surface area of $15\ m^2$. Using the given reflectivity of the lamp reflector and the viewing factor determined by geometry of the test setup an irradiance of $I = 1.83\ kW/m^2$ is calculated. From equation 2 an equilibrium temperature of $T_E = 83^\circ C$ is determined in good agreement with the experimental results.

The panel temperature distribution at the end of the cold phases is measured in the range $-158 \pm 5^\circ C$ for solar simulation cycling tests with one and with three panels and for infrared simulation tests with one and with three panels.

2.2 Temperature Changing Rates

During transition from warmphase to coldphase the temperature changing rates $\Delta T_p/\Delta t$ for solar simulation and for infrared simulation were measured as indicated in Table III. There is no essential difference in the temperature changing rates of solar simulation and infrared simulation in the temperature range $T_p > 50^\circ C$ to $T_p = -50^\circ C$. For a panel temperature of $T_p = -150^\circ C$ the temperature changing rate for infrared simulation is by a factor of 2 lower than the rate for solar simulation. In this temperature range the influence of structure parts of the lamp array modules which are not completely covered by the shutter has to be considered.

2.3 Cost effectiveness

The primary test cost saving effect can be achieved by simultaneous testing of three instead of one solar panel. Using a solar simulation facility and a multipanel test rig for three solar panels the operational test costs per panel amount to approximately 40 % of the costs for single panel testing. With a setup of infrared lamp array modules for three panels the operational test costs per panel are about 38 % of the operational costs for single panel solar simulation testing.

3. CONCLUSIONS

The comparison of multipanel thermal testing data for solar simulation and infrared simulation with single panel testing data indicate that the essential thermal cycling test requirements can be fulfilled for the two multipanel testing methods.

During an operational time of approximately 1.000 hours for the infrared lamp array modules including an LN2-cooled shutter no essential operational problems occurred and, therefore, the reliability of the system is promising.

In cases where no spectral match and no low collimation angle of the radiation are required infrared simulation thermal cycling of solar panels is advantageous because of cost effectiveness of multiple panel testing, high efficiency of infrared radiation setups and high life time of radiators.

REFERENCES

1. Skinner,D.J.; Wallin,S.P.; Wolff,C.M.: The Design and Application of an Infrared Simulator for Thermal Vacuum Testing, NASA SP-298, 1972, p. 197.

2. Dewey,R.L.: Control of an Artificial Infrared Environment to Simulate Complex, Time-Varying Orbital Conditions, NASA SP-298, 1972, p. 217.

3. Nelson,L.A.; Levine,M.B.: Development of a Heater Post and Spotlight Array for Thermal Vacuum Testing of the INTELSAT V Communication Satellite, NASA SP-336, 1973, p. 663.

4. Williams,F.U.: Analysis of Radiative Sources with Both Specular and Diffuse Characteristics in the Visible and Infrared Spectrum, NASA SP-379, 1975, p. 355.

5. Levine,M.B.; Nelson,L.A.: Development of a Carbon Cloth Heat Post Module for Thermal Vacuum Testing of a Spinning Spacecraft, NASA SP-298, 1972, p. 555.

6. Skinner,D.J.; Breiby,J.E.: The Design and Operation of an Infrared Simulator for Testing of the Shuttle Radiator System, NASA SP-336, 1973, p. 679.

7. Gülpen,J.; Lorenz,W.: Infrared Test Techniques Developed for the Helios Spacecraft, ESA SP-95, 1973, p. 301.

8. Esposti,P.L.D.; Strom,B.: Experimental Comparison between Infrared and Solar Simulation Test Philosophies in the Light of the Tests carried out on the Sirio Thermal Model, ESA SP-95, 1973, p. 263.

9. Arnoult,J.F.; Rollier,P.: Thermal Design Verification, Qualification and Acceptance Testing Concept for Future Large Space Objects, ESA-CR 3255/NL/77/HP(SC), 1977.

10. Prian,V.D.; Calimbas,A.T.; La Blanc,E.A.: Space Thermal Simulation for Satellite Heat Transfer Design Evaluation, Proc.5th Internat.Conf.Heat Transfer, Soc.of Heat Transfer of Japan, 1974, p. 267.

11. Ziermann,C.A.: A Comparison of Solar Beam and Infrared Simulation During Spacecraft Thermal Vacuum Testing, Proc. IES, 3rd Aerospace Testing Seminar, 1976, p. 67.

12. Schmidt,W.F.: A Comparison of Test Philosophies for Spacecraft Thermal Vacuum Testing, Proc.IES, 3rd Aerospace Testing Seminar, 1976, p. 73.

13. Weydandt,J.; Schwarz,B: Study of Thermal Design Verification, Qualification and Acceptance Testing Concept for Future Large Space Objects, ESA-CR 3199/NL/77/HP(SC), 1977.

14. Brinkmann,P.W.; Shickle,W.A.; Walker,J.B.: Economic Use of Facilities for Thermal Testing of Large Satellites and Subsystems, ESA SP-139, 1978, p. 387.

15. Schneider,K.: OTS Solar Array, ESA-SP 140, 1978, p. 193.

16. Nuss,H.: Calibration and Characteristic Measurements of a Solar Simulator Facility for Thermal Balance Tests, ESA SP-95, 1973, p. 137.

17. Brodersen,H.; Rizos,I.: INTELSAT V Solar Array, ESA SP-140, 1978, p. 209.

18. Reimann,J.: Facility for High Intensity, Thermal Balance Testing Using the Infrared Canister Method, ESA SP-95, 1973, p. 335.

19. Schneider,K.: Development and Testing of ULP Solar Array, ESA SP-140, 1978, p. 231.

20. Nuss, H.: Thermal Vacuum Testing of Solar Panels by Solar Simulation and Infrared Simulation, Proceedings IES of the 25th Technical Annual Meeting, Seattle, 1979, p. 188.

21. Brinkmann,P.W.; Reimann,J.: Efficient Thermal Cycling of Solar Panels in Solar Simulation Facilities with a Multi-Panel Test Rig, ESA/DFVLR, Second European Symposium on Photovoltaic Generators in Space, 15-17 April 1980.

22. Fokker-VFW, Space Division, Document ECS/057/PRO/0028/FOK and ECS/057/PRO/0034/FOK.

Table I: Test Requirements for Solar Panel Thermal Cycling Tests (ref. 15, 17, 19, 22)

Programme	Test Method	P mbar	I_{SC}	T_w °C	T_c °C	n_c	t_w min	t_c min	n_p	Additional Requirements
OTS/MAROTS										
Qualification	Solar	$1 \cdot 10^{-5}$	1 ± 0.03			50	93	117	1	Equilibrium criterion: $\Delta I/\Delta t \le 3$ °C/hour
Acceptance	Simulation	$1 \cdot 10^{-5}$	1 ± 0.03			10	93	117	1	
ECS/MARECS										
Qualification	Solar	$1 \cdot 10^{-4}$	1.26 ± 0.04		appr.-17?	50	30	150	1	Adjust solar irradiance to a value I equivalent to an open voltage of $64.1 \pm 0.?$ V
Acceptance	Simulation	$1 \cdot 10^{-4}$	1.08 ± 0.04		appr.-170	10	30 ± 3	90 ± 3	3	
ULP										
Qualification	Infrared Simulation	$1 \cdot 10^{-5}$		70 ± 10	-170 ± 10	20	80	250	1	Transition coldphase to warmphase: $\Delta I/\Delta t \le 10$ °C/min
INTELSAT V										
Qualification	Infrared	$1 \cdot 10^{-5}$		90 ± 5	-170 ± 5	35	100	188	1	Equilibrium criterion for mean value of reference thermocouples
Acceptance	Simulation	$1 \cdot 10^{-5}$		85 ± 5	-170 ± 5	7	100	188	3	

P : Chamber pressure

I : Irradiance of solar simulator in testplane

T_w, T_c : Equilibrium temperature of panels during warmphase and coldphase, respectively

t_w, t_c : Duration of warmphase and coldphase, respectively
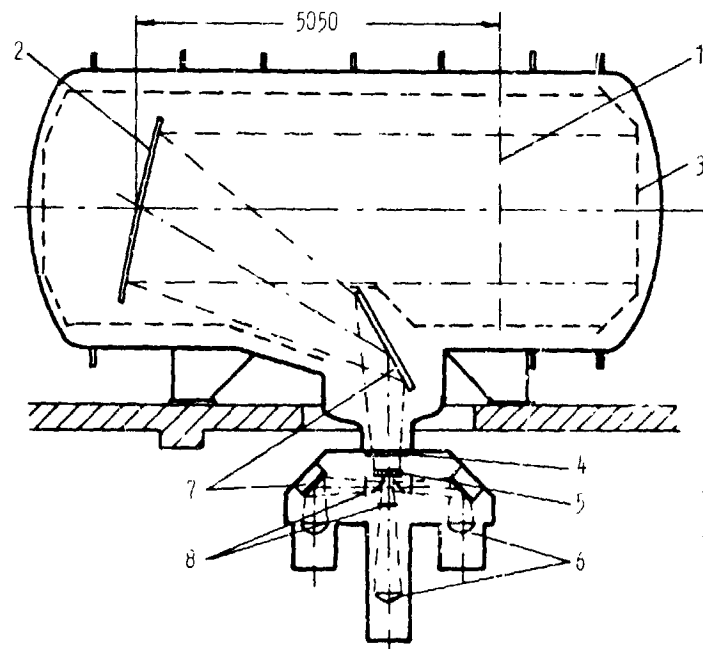
n_c : Number of cycles

n_p : Number of panels per test

Fig. 1: 3m-Space Simulation Facility
with Solar Simulator

1   Reference plane
2   Collimating mirror
3   Cold shroud
4   Quartz window
5   Integrator
6   Collector with high pressure
    Xenon lamp
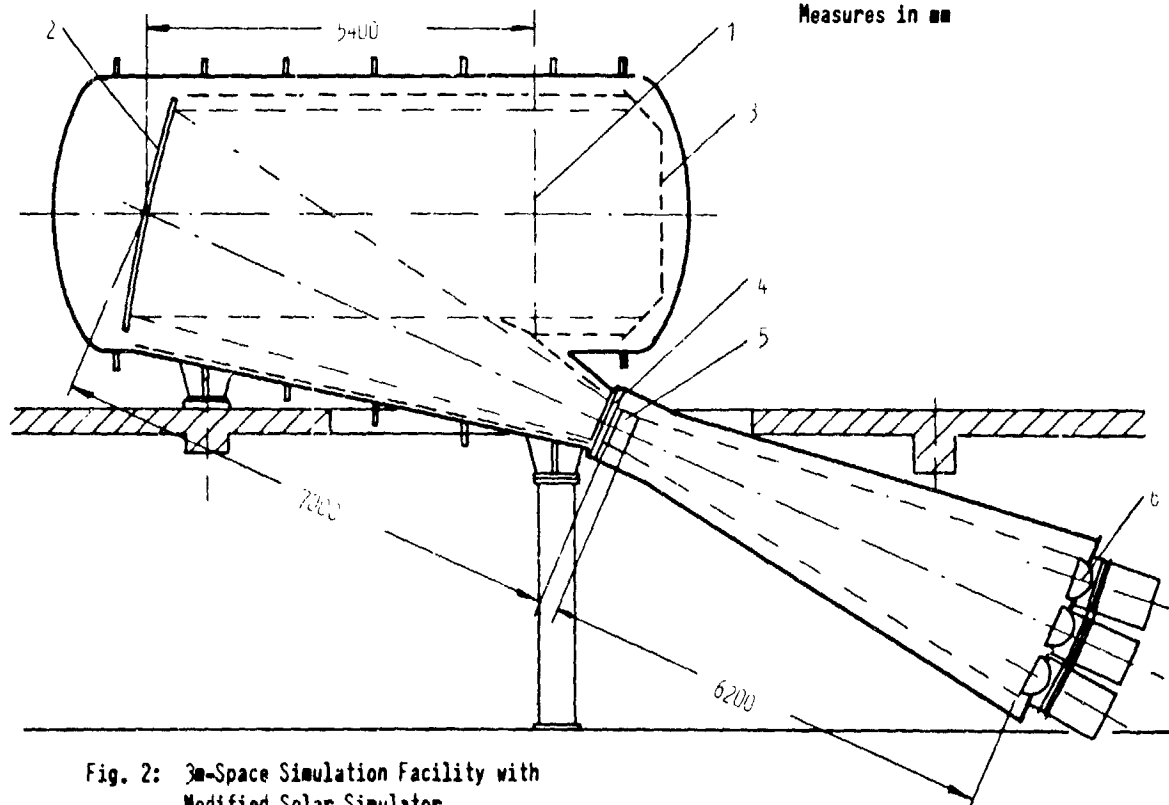7   Folding mirrors
8   Filters

Measures in mm

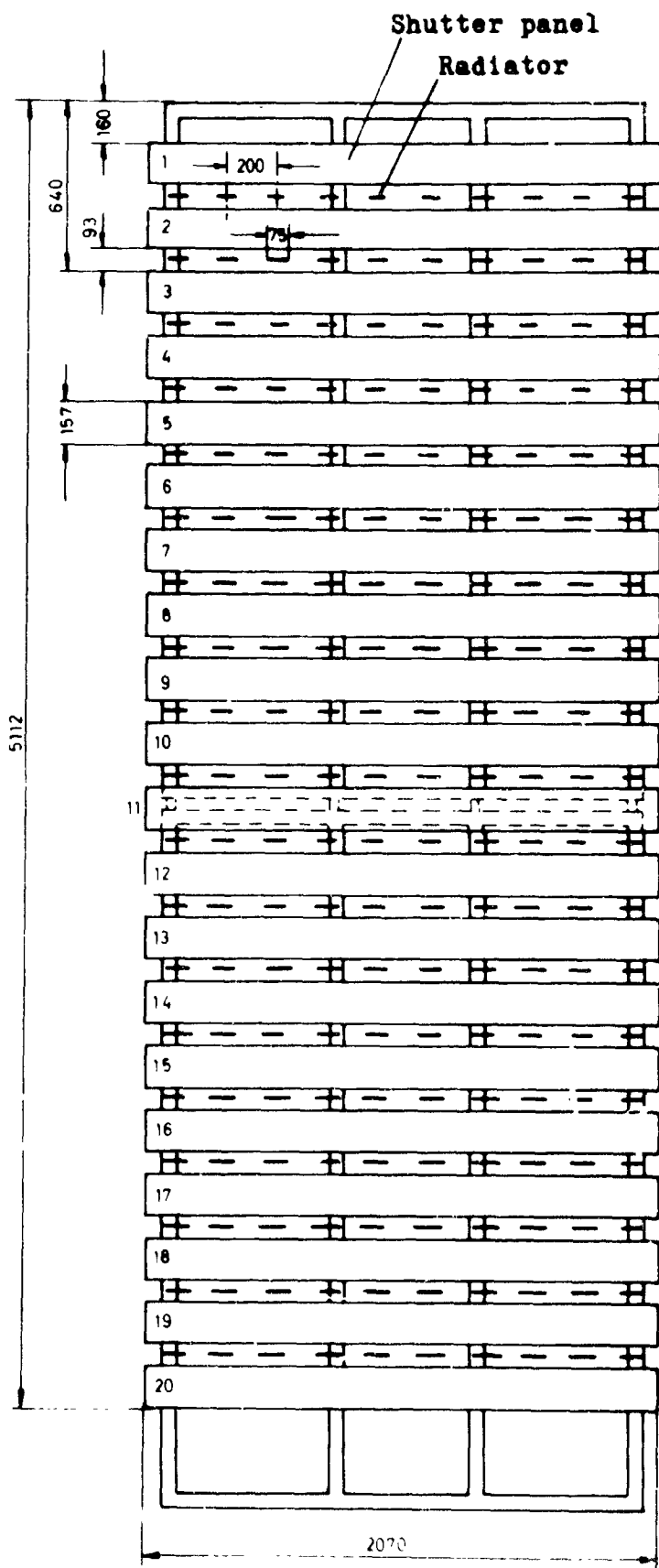Fig. 2: 3m-Space Simulation Facility with
Modified Solar Simulator

Fig. 3: Two Infrared Lamp Array Modules with Shutter Panels

Table II:

Number of extreme values n_e which show deviations from the mean value of

$$100 \ \frac{I_i - I_M}{I_M}$$

I_i : local irradiance,

I_M : mean value of irradiance

n_e	$100 \ \dfrac{I_i - I_M}{I_M}$
568	$\pm \ 0\%$ to $\pm \ 5\%$
144	$> \pm \ 5\%$ to $\pm \ 7\%$
53	$> \pm \ 7\%$ to $\pm \ 10\%$

Fig. 5: Typical Irradiance Distribution
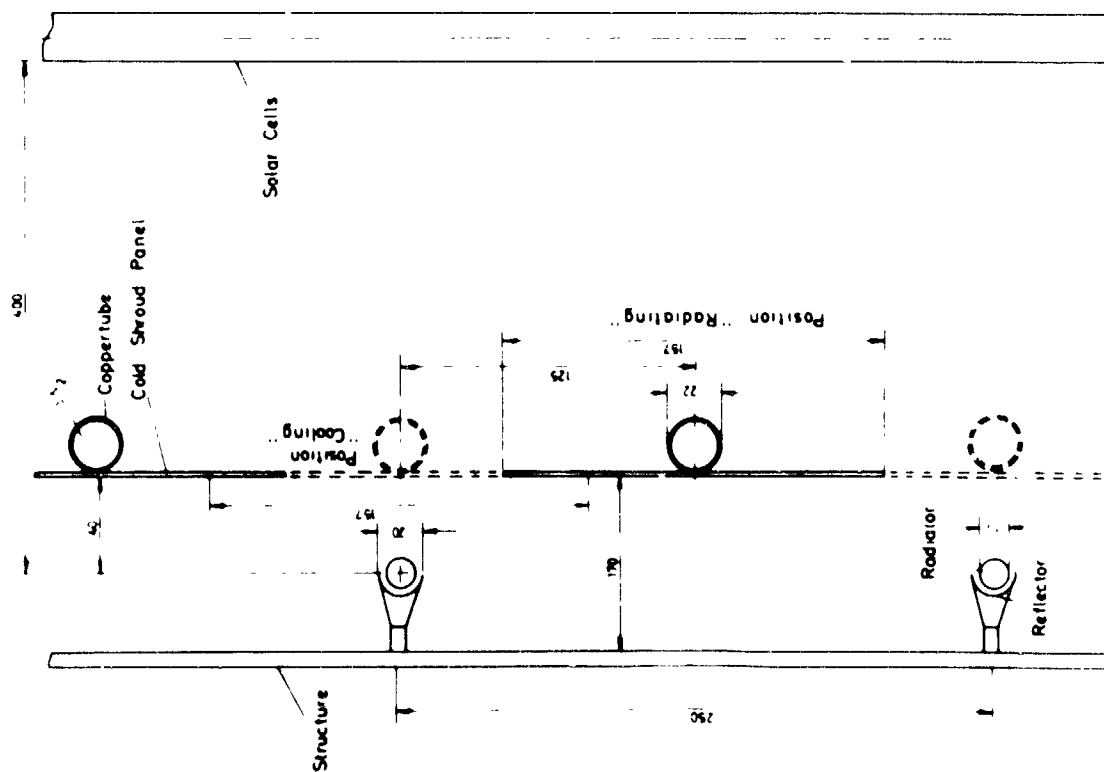
Fig. 4: Shutter Position during Warm- and Coldphase
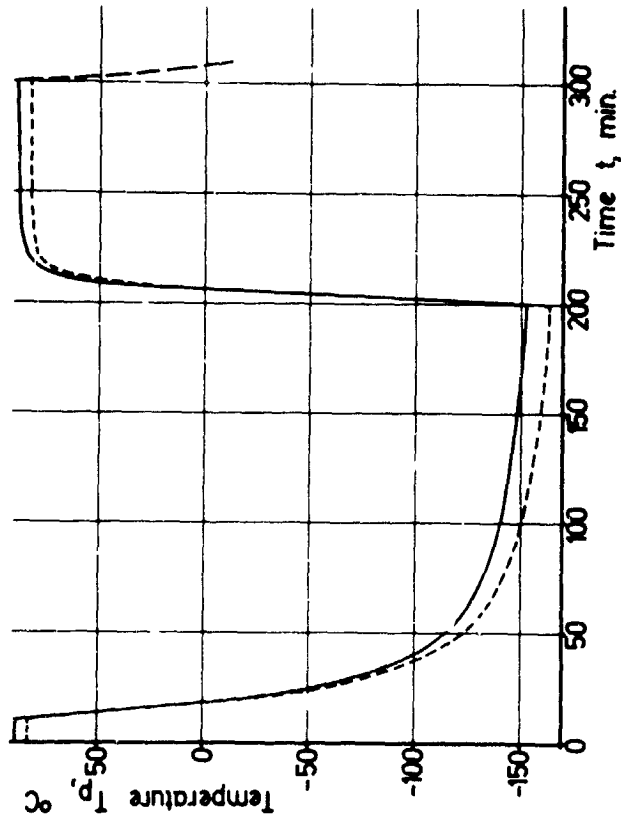
328

Fig.7: Typical Transient Phase of Infrared Simulation Cycling of Three Solarpanels.

T_p, °C	$\frac{\Delta T_p}{\Delta t}$ °C/min		f_m	f_c
	IR	Sol. Sim.		
- 50	6.5	7	1.08	1
- 100	1.9	2.3	1.21	1.1
- 150	0.2	0.4	2	2
- 155	0.03	0.3	10	10.4

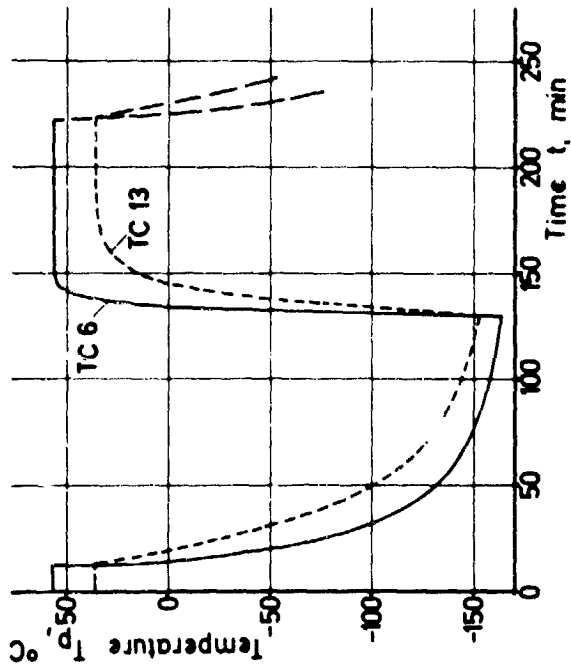Table III: Temperature changing rates

f_m: ratio measured

f_c: ratio calculated (equation 5)

Fig.6: Typical Transient Phase of Solar Simulation Cycling.
TC 6: Frontside Thermocouple; TC13: Rear Side Thermocouple

329